

Antikaon condensation in neutron stars by a new nonlinear mean-field model*

K. Miyazaki

Abstract

We have investigated both the K^- and \bar{K}^0 condensations in β -equilibrated neutron star (NS) matter using the relativistic mean-field model with the renormalized meson-baryon coupling constants. Adopting the antikaon optical potential of -120 MeV, our model predicts the K^- condensation as the second-order phase transition inside the neutron star of maximum mass, while the deeper potential than -160 MeV is ruled out. This is in contrast to the result of the density-dependent hadron field theory. Our model also predicts remarkable softening of the equation of state by the \bar{K}^0 condensation at high densities. Although this is contrasted with the result of the nonlinear Walecka model, only the K^- condensation can be formed in NSs.

1 Introduction

There recently is a considerable interest in the antikaon condensation that might be formed in dense nuclear medium as realized in high-energy heavy-ion collisions or in NSs. The relativistic mean-field (RMF) theory [1] has now been widely admitted to be suitable for describing such dense hadron matter [2]. Then the antikaon condensation in NSs has been investigated [3-7] by the so-called NLW models that include additional nonlinear self-coupling terms of mesons in the Walecka model. It is however noted that many parameters in the NLW model are adjusted to reproduce the properties of normal nuclear matter and finite nuclei. Therefore the NLW model is really valid at low densities, but there are no guarantees that it is useful at high densities where the antikaon condensation is expected to appear. In this respect the models embodying explicit or implicit density-dependence are desired. One of such efforts has been done in Ref. [8] using the density-dependent hadron field (DDRH) theory. However the DDRH model is based on the Dirac-Brueckner-Hartree-Fock (DBHF) theory [9], and there are no realistic DBHF calculations of baryon matter including hyperons at present in contrast to the nonrelativistic Brueckner-Hartree-Fock (NRBHF) theory [10,11]. As a result the density dependence of the meson-hyperon vertices in the DDRH model cannot be well determined.

Therefore the other RMF models, which exhibit density dependence but are independent of the DBHF theory, are desired. Zimanyi and Moszkowski (ZM) [12] developed

*This paper is the revised version of CDS ext-2004-036. Some texts and mistypes have been corrected.

one of such models. This model has the effective renormalized $NN\sigma$ coupling constant $g_{NN\sigma}^* = (M_N^*/M_N) g_{NN\sigma}$ where M_N^* is the effective mass of a nucleon in nuclear medium. It has been applied in Ref. [13] to K^- condensation in protoneutron stars. The ZM model however has the defect that it cannot reproduce the strong spin-orbit potentials because of its larger effective mass $M_N^* \simeq 0.86M_N$ than the reasonable value $M_N^* \simeq 0.6M_N$. Furthermore its extension to hyperons is ambiguous. Although Ref. [13] takes into account only nucleons as baryons, the realistic description of cold neutrino-free NS matter [14] requires all the baryon octets.

Recently, Ref. [15] has developed the model that is the generalization of the ZM model and can reproduce the nuclear matter saturation properties as well as the DBHF theory. Because it is based on the constituent quark picture of baryons, the effective renormalized meson-hyperon coupling constants are determined unambiguously. It has been applied to NS matter in Ref. [16]. The results of the particle composition and the mass-radius relation of NSs agree well with those obtained using the phenomenological but realistic effective equation-of-state (EOS) in Ref. [14]. The purpose of the present work is to extend the investigation of Ref. [16] by including the s-wave antikaon condensation. The characteristic feature of our model is that the effective renormalized meson-baryon coupling constants are determined self-consistently with the effective mass in the nuclear medium. This feature is also realized in the DBHF theory but not in the DDRH model. It is therefore worthwhile to compare our results with Ref. [8].

The detailed formulation of our model is essentially the same as Refs. [15] and [16] except for the antikaon contributions in antikaon condensed phase. Therefore we briefly summarize our formalism in the next section. In section 3 we first discuss the choices of the meson-baryon coupling constants and the antikaon optical potential, and then calculate the composition and the EOS of β -stable NS matter and the properties of NSs. Finally, the present study is summarized in the section 4.

2 Formalism

Our mean-field model Lagrangian for the baryons and leptons is the same as Ref. [16]. We consider the contributions of the isovector scalar meson δ [$a_0(980)$] and isovector vector meson ρ as well as the isoscalar scalar meson σ and isoscalar vector meson ω . The (hidden) strange mesons considered in Ref. [7] are not taken into account because the interactions between hyperons are not well known. For antikaons both the K^- and \bar{K}^0 of the isospin doublet are taken into account. The model Lagrangian for them is the same as Ref. [8] in which the free meson-kaon coupling constants have been used.

The formal expression of the energy density and pressure are common to every RMF models. (The DDRH model has additional rearrangement terms.)

$$\begin{aligned}
\mathcal{E} = & \frac{1}{4} \sum_{\substack{B=p,n,\Lambda,\Sigma^+, \\ \Sigma^0,\Sigma^-, \Xi^0, \Xi^-}} (3E_{BF}^* \rho_B + M_B^* \rho_{BS}) + \frac{1}{4} \sum_{l=e,\mu^-} (3E_{lF} \rho_l + m_l \rho_{lS}) + \sum_{\bar{K}=\bar{K}^0, K^-} m_{\bar{K}}^* \rho_{\bar{K}} \\
& + \frac{1}{2} m_\sigma^2 \langle \sigma \rangle^2 + \frac{1}{2} m_\omega^2 \langle \omega_0 \rangle^2 + \frac{1}{2} m_\delta^2 \langle \delta_3 \rangle^2 + \frac{1}{2} m_\rho^2 \langle \rho_{03} \rangle^2, \tag{1}
\end{aligned}$$

$$\begin{aligned}
P = & \frac{1}{4} \sum_{\substack{B=p,n,\Lambda,\Sigma^+, \\ \Sigma^0,\Sigma^-, \Xi^0, \Xi^-}} (E_{BF}^* \rho_B - M_B^* \rho_{BS}) + \frac{1}{4} \sum_{l=e,\mu^-} (E_{lF} \rho_l - m_l \rho_{lS}) \\
& - \frac{1}{2} m_\sigma^2 \langle \sigma \rangle^2 + \frac{1}{2} m_\omega^2 \langle \omega_0 \rangle^2 - \frac{1}{2} m_\delta^2 \langle \delta_3 \rangle^2 + \frac{1}{2} m_\rho^2 \langle \rho_{03} \rangle^2, \tag{2}
\end{aligned}$$

where ρ_B and ρ_l are the vector densities of the baryons and leptons in NS matter. E_{BF}^* and E_{lF} are their Fermi energies, and ρ_{BS} and ρ_{lS} are their scalar densities. The effective masses and density of the condensed antikaons [8] are $m_{\bar{K}}^*$ and $\rho_{\bar{K}}$. Each meson mean-fields are given by

$$\langle \sigma \rangle = - \frac{g_{nn\delta}^* (M_p^* - M_N) + g_{pp\delta}^* (M_n^* - M_N)}{g_{pp\sigma}^* g_{nn\delta}^* + g_{nn\sigma}^* g_{pp\delta}^*}, \tag{3}$$

$$\langle \delta_3 \rangle = \frac{g_{pp\sigma}^* (M_n^* - M_N) - g_{nn\sigma}^* (M_p^* - M_N)}{g_{pp\sigma}^* g_{nn\delta}^* + g_{nn\sigma}^* g_{pp\delta}^*}, \tag{4}$$

$$\langle \omega_0 \rangle = \sum_B \frac{g_{BB\omega}^*}{m_\omega^2} \rho_B - \sum_{\bar{K}} \frac{g_{K\bar{K}\omega}}{m_\omega^2} \rho_{\bar{K}}, \tag{5}$$

$$\langle \rho_{03} \rangle = \sum_B I_{3B} \frac{g_{BB\rho}^*}{m_\rho^2} \rho_B + \sum_{\bar{K}=\bar{K}^0, K^-} I_{3\bar{K}} \frac{g_{K\bar{K}\rho}}{m_\rho^2} \rho_{\bar{K}}, \tag{6}$$

where $I_{3B} = \{1, -1, 0, 1, 0, -1, 1, -1\}$ for $B = \{p, n, \Lambda, \Sigma^+, \Sigma^0, \Sigma^-, \Xi^0, \Xi^-\}$ and $I_{3\bar{K}} = \{1, -1\}$ for $\bar{K} = \{\bar{K}^0, K^-\}$.

The renormalized coupling constants of the nucleons are [17]

$$g_{pp\sigma(\omega)}^* = [(1 - \lambda_N) + \lambda_N m_p^*] g_{NN\sigma(\omega)}, \tag{7}$$

$$g_{nn\sigma(\omega)}^* = [(1 - \lambda_N) + \lambda_N m_n^*] g_{NN\sigma(\omega)}, \tag{8}$$

$$g_{pp\delta(\rho)}^* = [(1 - \lambda_N) + \lambda_N (2m_n^* - m_p^*)] g_{NN\delta(\rho)}, \tag{9}$$

$$g_{nn\delta(\rho)}^* = [(1 - \lambda_N) + \lambda_N (2m_p^* - m_n^*)] g_{NN\delta(\rho)}, \tag{10}$$

where $m_B^* = M_B^*/M_B$. The renormalized coupling constants of Λ are [15]

$$g_{\Lambda\Lambda\sigma(\omega)}^* = [(1 - \lambda_\Lambda) + \lambda_\Lambda m_\Lambda^*] g_{\Lambda\Lambda\sigma(\omega)}. \quad (11)$$

Similarly, for the Σ 's we have [16]

$$g_{\Sigma^+\Sigma^+\Pi}^* = [(1 - \lambda_\Sigma) + \lambda_\Sigma m_{\Sigma^+}^*] g_{\Sigma\Sigma\Pi}, \quad (12)$$

$$g_{\Sigma^0\Sigma^0\Pi}^* = [(1 - \lambda_\Sigma) + \lambda_\Sigma m_{\Sigma^0}^*] g_{\Sigma\Sigma\Pi}, \quad (13)$$

$$g_{\Sigma^-\Sigma^-\Pi}^* = [(1 - \lambda_\Sigma) + \lambda_\Sigma m_{\Sigma^-}^*] g_{\Sigma\Sigma\Pi}, \quad (14)$$

where $\Pi = \sigma, \omega, \delta$ and ρ but $g_{\Sigma^0\Sigma^0\delta(\rho)} = 0$. Although the meson- Ξ coupling constants are not renormalized in the present model [15] because of the absence of strange mesons, we formally introduce

$$g_{\Xi\Xi\Pi}^* = [(1 - \lambda_\Xi) + \lambda_\Xi m_\Xi^*] g_{\Xi\Xi\Pi}. \quad (15)$$

The renormalization constant λ_B is summarized by

$$\lambda_B = \begin{cases} 1/3 : S = 0, \\ 1/4 : S = -1, \\ 0 : S = -2. \end{cases} \quad (16)$$

where S is the strangeness of each baryon.

The effective mass of each hyperon m_Y^* is expressed by nucleon's mass $m_{p(n)}^*$. They are determined by solving the self-consistency equations $\partial\mathcal{E}/\partial m_p^* = 0$ and $\partial\mathcal{E}/\partial m_n^* = 0$ simultaneously:

$$\begin{aligned} & \sum_B \frac{\partial m_B^*}{\partial m_p^*} \frac{M_B}{M_N} \frac{\rho_{BS}}{\rho_T} + \sum_{\bar{K}} \frac{f_{\bar{K}}}{M_N} \frac{\partial m_{\bar{K}}^*}{\partial m_p^*} \\ & + \left(\frac{m_\sigma}{g_{NN\sigma}} \right)^2 \frac{M_N}{\rho_T} \frac{A^{(0)} \left(A_p^{(1)} C^{(0)} - A^{(0)} C_p^{(1)} \right)}{(C^{(0)})^3} + \left(\frac{m_\delta}{g_{NN\delta}} \right)^2 \frac{M_N}{\rho_T} \frac{B^{(0)} \left(C^{(0)} - B^{(0)} C_p^{(1)} \right)}{(C^{(0)})^3} \\ & + \left(\sum_B \lambda_B f_B \frac{g_{BB\omega}}{m_\omega} \frac{\partial m_B^*}{\partial m_p^*} \right) \left(\sum_B f_B \frac{g_{BB\omega}^*}{m_\omega} - \sum_{\bar{K}} f_{\bar{K}} \frac{g_{KK\omega}}{m_\omega} \right) \frac{\rho_T}{M_N} \\ & + \left(\sum_B I_{3B} \lambda_B f_B \frac{g_{BB\rho}}{m_\rho} \frac{\partial \tilde{m}_B^*}{\partial m_p^*} \right) \left(\sum_B I_{3B} f_B \frac{g_{BB\rho}^*}{m_\rho} + \sum_{\bar{K}} I_{3\bar{K}} f_{\bar{K}} \frac{g_{KK\rho}}{m_\rho} \right) \frac{\rho_T}{M_N} = 0, \quad (17) \end{aligned}$$

$$\begin{aligned}
& \sum_B \frac{\partial m_B^*}{\partial m_n^*} \frac{M_B}{M_N} \frac{\rho_{BS}}{\rho_T} + \sum_{\bar{K}} \frac{f_{\bar{K}}}{M_N} \frac{\partial m_{\bar{K}}^*}{\partial m_n^*} \\
& + \left(\frac{m_\sigma}{g_{NN\sigma}} \right)^2 \frac{M_N}{\rho_T} \frac{A^{(0)} \left(A_n^{(1)} C^{(0)} - A^{(0)} C_n^{(1)} \right)}{(C^{(0)})^3} - \left(\frac{m_\delta}{g_{NN\delta}} \right)^2 \frac{M_N}{\rho_T} \frac{B^{(0)} \left(C^{(0)} + B^{(0)} C_n^{(1)} \right)}{(C^{(0)})^3} \\
& + \left(\sum_B \lambda_B f_B \frac{g_{BB\omega}}{m_\omega} \frac{\partial m_B^*}{\partial m_n^*} \right) \left(\sum_B f_B \frac{g_{BB\omega}^*}{m_\omega} - \sum_{\bar{K}} f_{\bar{K}} \frac{g_{KK\omega}}{m_\omega} \right) \frac{\rho_T}{M_N} \\
& + \left(\sum_B I_{3B} \lambda_B f_B \frac{g_{BB\rho}}{m_\rho} \frac{\partial \tilde{m}_B^*}{\partial m_n^*} \right) \left(\sum_B I_{3B} f_B \frac{g_{BB\rho}^*}{m_\rho} + \sum_{\bar{K}} I_{3\bar{K}} f_{\bar{K}} \frac{g_{KK\rho}}{m_\rho} \right) \frac{\rho_T}{M_N} = 0, \quad (18)
\end{aligned}$$

where f_B and $f_{\bar{K}}$ are the ratios of each baryon and antikaon densities to the total baryon density ρ_T . Various quantities in Eqs. (17) and (18) were given in Ref. [16] except for antikaon contributions:

$$\frac{\partial m_{\bar{K}}^*}{\partial m_p^*} = \frac{r_{K\sigma} \left(A_p^{(1)} C^{(0)} - A^{(0)} C_p^{(1)} \right) + r_{K\delta} I_{3K} \left(C^{(0)} - B^{(0)} C_p^{(1)} \right)}{(C^{(0)})^2} M_N, \quad (19)$$

$$\frac{\partial m_{\bar{K}}^*}{\partial m_n^*} = \frac{r_{K\sigma} \left(A_n^{(1)} C^{(0)} - A^{(0)} C_n^{(1)} \right) - r_{K\delta} I_{3K} \left(C^{(0)} + B^{(0)} C_n^{(1)} \right)}{(C^{(0)})^2} M_N, \quad (20)$$

where $r_{K\sigma(\delta)} = g_{KK\sigma(\delta)}/g_{NN\sigma(\delta)}$.

3 Numerical analyses

For numerical calculations of NS matter, we first determine the free meson-baryon coupling constants. The $NN\sigma$ and $NN\omega$ coupling constants are fixed [15] to reproduce the nuclear matter saturation properties. We assume the saturation energy of -15.75 MeV at the saturation density 0.16 fm^{-3} . The values of $(g_{NN\sigma}/m_\sigma)^2 = 16.9 \text{ fm}^2$ and $(g_{NN\omega}/m_\omega)^2 = 12.5 \text{ fm}^2$ are obtained. The effective nucleon mass and the incompressibility of saturated nuclear matter are $m_N^* = 0.605$ and $K = 302 \text{ MeV}$ respectively. The $YY\omega$ coupling constants are fixed from the SU(6) symmetry:

$$\frac{1}{3} g_{NN\omega} = \frac{1}{2} g_{\Lambda\Lambda\omega} = \frac{1}{2} g_{\Sigma\Sigma\omega} = g_{\Xi\Xi\omega}. \quad (21)$$

The $YY\sigma$ coupling constants are determined to give the hyperon potentials $U_Y^{(N)}$ in saturated nuclear matter for which we take the same values as Ref. [8]:

$$U_\Lambda^{(N)} = -30 \text{ MeV}, \quad U_\Sigma^{(N)} = 30 \text{ MeV} \quad \text{and} \quad U_\Xi^{(N)} = -18 \text{ MeV}. \quad (22)$$

In our model they are given by

$$U_Y^{(N)} = -g_{YY\sigma}^* \langle \sigma \rangle_{NM} + g_{YY\omega}^* \langle \omega_0 \rangle_{NM}, \quad (23)$$

where $\langle \sigma \rangle_{NM}$ and $\langle \omega_0 \rangle_{NM}$ are the mean-fields in saturated nuclear matter.

Although the calculated symmetry energy of nuclear matter becomes smaller (24.6 MeV) than the empirical value 30 ± 4 MeV, we employ the values of the Bonn A potential in Ref. [9], $(g_{NN\delta}/m_\delta)^2 = 0.39 \text{ fm}^2$ and $(g_{NN\rho}/m_\rho)^2 = 0.82 \text{ fm}^2$ for $NN\delta$ and $NN\rho$ coupling constants. The reason of such choices was discussed in Ref. [16]. The $YY\delta$ and $YY\rho$ coupling constants are also fixed from the SU(6) symmetry:

$$g_{NN\delta} = \frac{1}{2} g_{\Sigma\Sigma\delta} = g_{\Xi\Xi\delta} \quad \text{and} \quad g_{\Lambda\Lambda\delta} = 0, \quad (24)$$

$$g_{NN\rho} = \frac{1}{2} g_{\Sigma\Sigma\rho} = g_{\Xi\Xi\rho} \quad \text{and} \quad g_{\Lambda\Lambda\rho} = 0. \quad (25)$$

Finally, we have to determine the meson-(anti)kaon coupling constants. The isoscalar vector coupling is derived from quark model as

$$g_{KK\omega} = \frac{1}{3} g_{NN\omega}. \quad (26)$$

Similarly, the isovector meson couplings are

$$g_{KK\delta} = g_{NN\delta} \quad \text{and} \quad g_{KK\rho} = g_{NN\rho}. \quad (27)$$

The remaining σ -meson coupling is usually determined [3-7] from the given K^- optical potential at saturated nuclear matter density:

$$U_{\bar{K}}(\rho_0) = -g_{KK\sigma} \langle \sigma \rangle_{NM} - g_{KK\omega} \langle \omega_0 \rangle_{NM}. \quad (28)$$

We further need to fix the value of $U_{\bar{K}}(\rho_0)$ in Eq. (28). Recently, many efforts to derive this value have been done. Reference [18] has determined $g_{KK\sigma(\omega)}$ by matching the relativistic mean-field potential in nuclear interior to the phenomenological density-dependent potential fitted to K^- atomic data in nuclear surface, and then the rather deep potential $U_{\bar{K}}(\rho_0) \approx -180$ MeV is obtained. However the $U_{\bar{K}}(\rho_0)$ at nuclear center cannot be uniquely determined from K^- atomic data even with high precision because K^- atomic data give information only on the far outer region of the potential. Therefore the direct theoretical calculations of $U_{\bar{K}}(\rho_0)$ are expected. In fact the coupled-channel Lippmann-Schwinger calculations [19-21] based on the effective chiral model have been done and yielded shallower potentials $U_{\bar{K}}(\rho_0) = -100 \text{ MeV} \sim -120 \text{ MeV}$. Furthermore, more refined self-consistent calculations [22,23], in which the K^- optical potential should be incorporated in the in-medium K^- propagator, generate much shallower potentials

$$U_{\bar{K}}(\rho_0) = -55 \text{ MeV} \sim -66 \text{ MeV}.$$

Here we should note the two points: The first is that the K^- condensation in β -stable NS matter appears at much higher density than the normal nuclear matter density ρ_0 . This indicates that a relevant quantity to the \bar{K} condensations is $U_{\bar{K}}(\rho)$ at higher density rather than $U_{\bar{K}}(\rho_0)$. Because our effective meson-baryon coupling constants are renormalized, it is proper to introduce the renormalized (or implicitly density-dependent) meson-kaon coupling constants. If they have strong density-dependences, the $U_{\bar{K}}(\rho_0)$ cannot give us precise information on the optical potential of condensed kaons. In our model the renormalized meson-kaon coupling constants can be introduced by taking into account the mean-fields of the (hidden) strange mesons and will be studied in future works. The second is that the coupled-channel calculations are not consistent with the RMF models of nuclear matter. The most important difference is the largely reduced masses of the baryons in the RMF models that are not incorporated in the investigations of Refs. [19-23]. This suggests that the above values of $U_{\bar{K}}(\rho_0)$ cannot be used in the RMF models without any modifications. These problems might be resolved by the DBHF calculation containing full meson-baryon channels, but that is not feasible at present.

In spite of the above problems, we have three classes of the antikaon optical potential in any way, the shallowest one $U_{\bar{K}}(\rho_0) \simeq -60 \text{ MeV}$, the deepest one $U_{\bar{K}}(\rho_0) \simeq -180 \text{ MeV}$ and the middle value $U_{\bar{K}}(\rho_0) \simeq -120 \text{ MeV}$ between the two. If the shallowest potential is in fact, the antikaon condensation cannot be expected in the NS matter. We therefore choose the medium value $U_{\bar{K}}(\rho_0) = -120 \text{ MeV}$ for the first time. In this case the $KK\sigma$ coupling constant $g_{KK\sigma}/g_{NN\sigma} = 1.4 \times 10^{-2}$ derived from Eq. (28) is negligibly small and so the KK interaction is the vector current interaction. This is consistent to the coupled channel calculations [20] of the antikaon optical potential. The same result is also found in the DDRH model [8] using the Groningen potential whereas the NLW model using the GM parameter set [7] have non-negligible scalar interaction.

Figure 1 shows the particle compositions of the cold β -stable NS matter as functions of the total baryon density, which are obtained by solving the β -equilibrium condition, the baryon number conservation and the charge neutrality condition as well as Eqs. (17) and (18) in a self-consistent way. At low densities the matter consists of nucleons and leptons. The μ^- appears near the saturation density $\rho_T = 0.169 \text{ fm}^{-3}$. The Λ appears above $\rho_T = 0.373 \text{ fm}^{-3}$ and the Ξ^- stands immediately after Λ at $\rho_T = 0.421 \text{ fm}^{-3}$. As soon as the Ξ^- increases, the fractions of the leptons are depleted because of the charge neutrality condition and the fraction of neutron begins to decrease gently. The K^- condensation is formed above $\rho_T = 0.653 \text{ fm}^{-3}$ and so the Ξ^- turns to decrease because of the charge neutrality. The Ξ^0 appears above $\rho_T = 0.880 \text{ fm}^{-3}$ and as a result the Ξ^- decreases more rapidly because of the baryon number conservation.

After the \bar{K}^0 condensation is formed at $\rho_T = 1.038 \text{ fm}^{-3}$, the Ξ^- turns to increase again whereas the increases of K^- and Ξ^0 become gentle. Consequently, the baryon fraction becomes nearly isospin symmetric as has been explained in Ref. [6]. When the electron

vanishes at $\rho_T = 1.315 \text{ fm}^{-3}$, the β -equilibrium conditions containing the electrochemical potential lose their proper meanings. (The μ^- has already vanished at $\rho_T = 0.842 \text{ fm}^{-3}$.) Alternatively, the NS matter is constrained by the isospin-saturated symmetry of the baryon and antikaon fractions. This phenomenon has been also seen in Ref. [8]. Above $\rho_T = 1.315 \text{ fm}^{-3}$ the electrochemical potential becomes negative, that is, the positrons appear in place of electrons. Because the positron is scarce $\rho_{e^+} < 1.0 \times 10^{-4} \text{ fm}^{-3}$, it is not shown in Fig. 1. However it is apparent in the fact that above $\rho_T = 1.315 \text{ fm}^{-3}$ the fraction of Ξ^- becomes slightly larger than Ξ^0 because of the charge neutrality. We stopped the calculation when the effective mass of the neutron becomes negative at $\rho_T = 1.393 \text{ fm}^{-3}$. The Σ hyperons never appear in Fig. 1 because of their repulsive optical potential in Eq. (22). The proton distribution has two apparent kinks over the range of ρ_T , which correspond to the appearances of Ξ^- and K^- because the proton is only one particle with positive charge. On the other hand, the neutral baryon Λ increases smoothly as the total baryon density grows.

The solid curve in Fig. 2 shows the EOS corresponding to Fig. 1. The dashed and dotted curves are the results with only K^- and no \bar{K} condensations. In this case the antikaon condensations are formed as the second-order phase transitions. The solid curve shows three kinks: The first one corresponds to the appearance of Λ hyperons. The second and third ones correspond to the phase transition to K^- and \bar{K}^0 condensed phases. As is well known, the antikaon condensations soften the EOS. The effect of the \bar{K}^0 condensation is much stronger than the K^- condensation. This is also seen in the DDRH model of Ref. [8] but not in the NLW models of Ref. [7]. We therefore see that the remarkable softening of the EOS by the \bar{K}^0 condensation is characteristic to the RMF models containing the explicit (DDRH) or implicit (ours) density-dependences of the meson-baryon coupling constants.

We next choose the deeper antikaon optical potential $U_{\bar{K}}(\rho_0) = -155 \text{ MeV}$ for which the $KK\sigma$ coupling constant is still small $g_{KK\sigma}/g_{NN\sigma} = 9.6 \times 10^{-2}$. The EOS is shown in Fig. 3. The dashed and dotted curves are the results with only K^- and no \bar{K} condensations. In this case the antikaon condensations appear as the first-order phase transitions. We employ the Maxwell construction to determine the equilibrium state or the mixed phase of two phases, the pure baryon and K^- -condensed phases, or the K^- and \bar{K}^0 condensed phases. The pressure at the phase transition is determined by seeking a point of intersection in the correlation between the pressure P and the Gibbs free energy per baryon \bar{G} . As a result of the first-order phase transition, $\partial\bar{G}/\partial P$ is discontinuous at the transition point. Recently, another construction of the equilibrium state between the pure baryon and the K^- condensed phases, which requires that the pressure, baryochemical μ_n and electrochemical μ_e potentials are the same in the two phases but relaxes the constraint of the local charge neutrality in each of the two phases to the global neutrality of the mixed phase, is proposed in Ref. [5] and has been used in Refs. [7] and [13]. We have however used the Maxwell construction because our

calculation includes both \bar{K}^0 and K^- condensations simultaneously [6] and because the breaking of local charge neutrality induces additional structure in the medium that is essentially beyond the mean-field theory. The red dotted lines in Fig. 3 show the mixed phases due to the Maxwell construction. It is seen again that the \bar{K}^0 condensation softens the EOS remarkably.

For the deeper antikaon optical potentials of $|U_{\bar{K}}(\rho_0)| \geq 160$ MeV, the Maxwell construction cannot be applied to the \bar{K}^0 condensation because the effective mass of the neutron becomes negative before we arrive at a point of intersection in the correlation between P and \bar{G} . Namely, the deepest antikaon optical potential $U_{\bar{K}}(\rho_0) \approx -180$ MeV mentioned above is not allowed in our model. This feature of our model is again contrasted to the NLW models [7] that do not exclude the deepest potential.

Using the EOS obtained above, we calculate the mass sequences and the mass-radius relations of non-rotating NSs in Figs. 4 and 5 by integrating the Tolman-Oppenheimer-Volkov equation [24]. For the outer region of NSs, we use the EOS by Feynman-Metropolis-Teller, Baym-Pethick-Sutherland and Negele-Vautherin from Ref. [25]. The dotted curves are the results with no \bar{K} condensations. The maximum mass is $1.736M_\odot$, $1.524M_\odot$ and $1.749M_\odot$ for $U_{\bar{K}}(\rho_0) = -120$ MeV, $U_{\bar{K}}(\rho_0) = -155$ MeV and no \bar{K} respectively. The corresponding radius is 12.51 km, 13.19 km and 12.14 km respectively. The difference between the results with $U_{\bar{K}}(\rho_0) = -120$ MeV and no \bar{K} is small because the \bar{K} condensations suppress the abundances of Ξ hyperons as seen in Fig. 1. The central density of the maximum mass star for $U_{\bar{K}}(\rho_0) = -120$ MeV is $\rho_T \approx 0.81 \text{ fm}^{-3}$. From Fig. 1 we can therefore see that there are no \bar{K}^0 condensations in neutron stars. For $U_{\bar{K}}(\rho_0) = -155$ MeV the plateaus on the both sides of the maximum in Fig. 4 correspond to the mixed state due to K^- and \bar{K}^0 condensations by the Maxwell construction. Again there are no \bar{K}^0 condensations in NSs. The \bar{K}^0 condensation is also ruled out in the DDRH model of Ref. [8]. In the NLW model [7] it is able to appear in the third family of compact stars. In the DDRH model [8] the K^- condensation is formed inside the maximum mass stars only for $|U_{\bar{K}}(\rho_0)| \geq 160$ MeV while in our model such deep antikaon optical potentials are ruled out and the K^- condensation already appears for $U_{\bar{K}}(\rho_0) = -120$ MeV. This is the striking difference between our and the DDRH model. We here note that our meson- Ξ coupling constants are not renormalized as seen in Eq. (16). The (hidden) strange mesons have to be taken into account to renormalize the meson- Ξ coupling constants in our model. However, so far as the DDRH model also has no effects by the strange mesons, the comparison between the two models is meaningful.

4 Summary

We have investigated both the K^- and \bar{K}^0 condensations in β -equilibrated NS matter using the RMF model with the renormalized meson-baryon coupling constants. Our model is the generalization of the ZM model based on the constituent quark picture of

baryons. For the antikaon optical potential $U_{\bar{K}}(\rho_0) = -120$ MeV the condensations are the second-order phase transitions while for the deeper potential $U_{\bar{K}}(\rho_0) = -155$ MeV they become the first-order transitions in which we have used the Maxwell construction for the mixed phases. Although the \bar{K}^0 condensation softens the EOS remarkably, only the K^- condensation is formed in the NS of maximum mass. This is unfortunate because the marked softening of EOS by the \bar{K}^0 condensation is intrinsic to the models embodying explicit (DDRH) or implicit (ours) density-dependent coupling constants. The much deeper potentials of $|U_{\bar{K}}(\rho_0)| \geq 160$ MeV are not allowed in our model because the Maxwell construction cannot be applied. This is in sharp contrast to the result of the DDRH model in which the K^- condensation is formed in NSs only using $|U_{\bar{K}}(\rho_0)| \geq 160$ MeV.

The existence of the antikaon condensation essentially depends on the depth of the antikaon optical potential. At present we have no reliable information on it. One of the serious theoretical problems is the density-dependence of the potential strength because the antikaon condensations occur in NSs at much higher density than the saturation density of normal nuclear matter. So as to investigate this problem, the future work will take into account the effects by the (hidden) strange mesons that introduce the renormalized meson- K as well as meson- Ξ coupling constants.

References

- [1] B.D. Serot and J.D. Walecka, *Advances in Nuclear Physics*, Vol. **16** (Plenum, New York, 1986).
- [2] N.K. Glendenning, *Astrophys. J.* **293** (1985) 470.
- [3] R. Knorren, M. Prakash and P.J. Ellis, *Phys. Rev.* **C52** (1995) 3470, [arXiv:nucl-th/9506016].
- [4] J. Schaffner and I.N. Mishustin, *Phys. Rev.* **C53** (1996) 1416, [arXiv:nucl-th/9506011].
- [5] N.K. Glendenning and J. Schaffner, *Phys. Rev.* **C60** (1999) 025803, [arXiv:astro-ph/9810290].
- [6] S. Pal, D. Bandyopadhyay and W. Greiner, *Nucl. Phys.* **A674** (2000) 553, [arXiv:astro-ph/0001039].
- [7] S. Banik and D. Bandyopadhyay, *Phys. Rev.* **C64** (2001) 055805, [arXiv:astro-ph/0106406].
- [8] S. Banik and D. Bandyopadhyay, *Phys. Rev.* **C66** (2002) 065801, [arXiv:astro-ph/0205532].
- [9] R. Brockmann and R. Machleidt, *Phys. Rev.* **C42** (1990) 1965.
- [10] M. Baldo, G.F. Burgio and H.-J. Schulze, *Phys. Rev.* **C61** (2000) 055801, [arXiv:nucl-th/9912066].
- [11] I. Vidaña, A. Polls, A. Ramos, L. Engvik and M. Hjorth-Jensen, *Phys. Rev.* **C62** (2000) 035801, [arXiv:nucl-th/0004031].
- [12] J. Zimanyi and S.A. Moszkowski, *Phys. Rev.* **C42** (1990) 1416. It is noted that the NLW model has linear meson-baryon couplings in spite of its name. On the contrary, the ZM model is true nonlinear mean-field model.
- [13] J.A. Pons, S. Reddy, P.J. Ellis, M. Prakash and J.M. Lattimer, *Phys. Rev.* **C62** (2000) 035803, [arXiv:nucl-th/0003008].
- [14] S. Balberg, I. Lichtenstadt and G.B. Cook, *Astrophys. J. Suppl.* **121** (1999) 515.
- [15] K. Miyazaki, CERN Document Server (CDS) ext-2003-062 revised by Mathematical Physics Preprint Archive (mp_arc) 05-178.
- [16] K. Miyazaki, CERN Document Server (CDS) ext-2004-010 revised by Mathematical Physics Preprint Archive (mp_arc) 05-199.

- [17] K. Miyazaki, CERN Document Server (CDS) ext-2003-077 revised by Mathematical Physics Preprint Archive (mp_arc) 05-190.
- [18] E. Friedman, A. Gal, J. Mareš and A. Cieplý, Phys. Rev. **C60** (1999) 024314, [arXiv:nucl-th/9804072].
- [19] V. Koch, Phys. Lett. **B337** (1994) 7.
- [20] T. Waas and W. Weise, Nucl. Phys. **A625** (1997) 287.
- [21] A. Ramos and E. Oset, arXiv:nucl-th/9810014.
- [22] A. Ramos and E. Oset, Nucl. Phys. **A671** (2000) 481.
- [23] A. Cieplý, E. Friedman, A. Gal and J. Mareš, Nucl. Phys. **A696** (2001) 173,
- [24] W.D. Arnett and R.L. Bowers, Astrophys. J. Suppl. **33** (1977) 415.
- [25] V. Canuto, Ann. Rev. Astr. Ap. **12** (1974) 167; **13** (1975) 335.

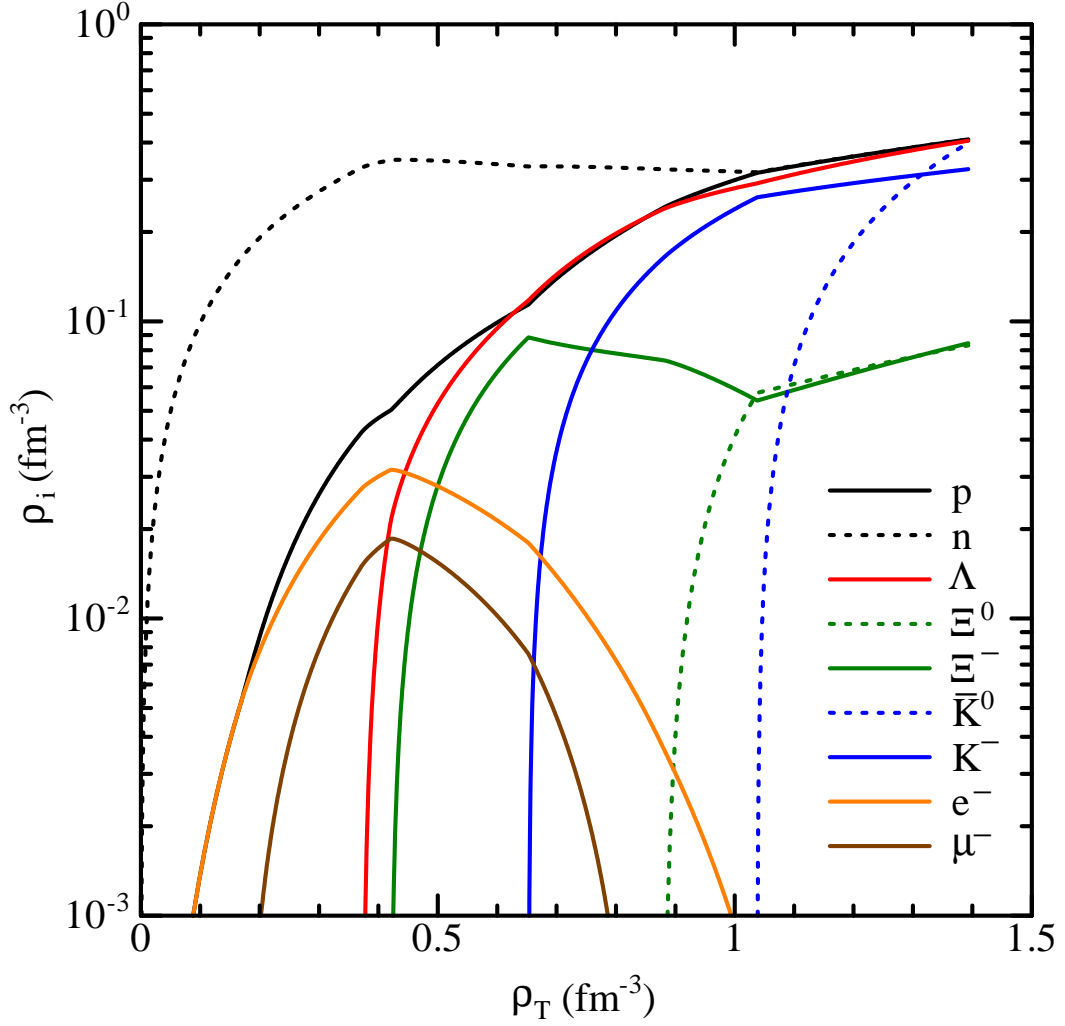


Figure 1: The particle compositions of the cold β -stable NS matter using the K^- optical potential $U_{\bar{K}}(\rho_0) = -120 \text{ MeV}$ as functions of the total baryon density.

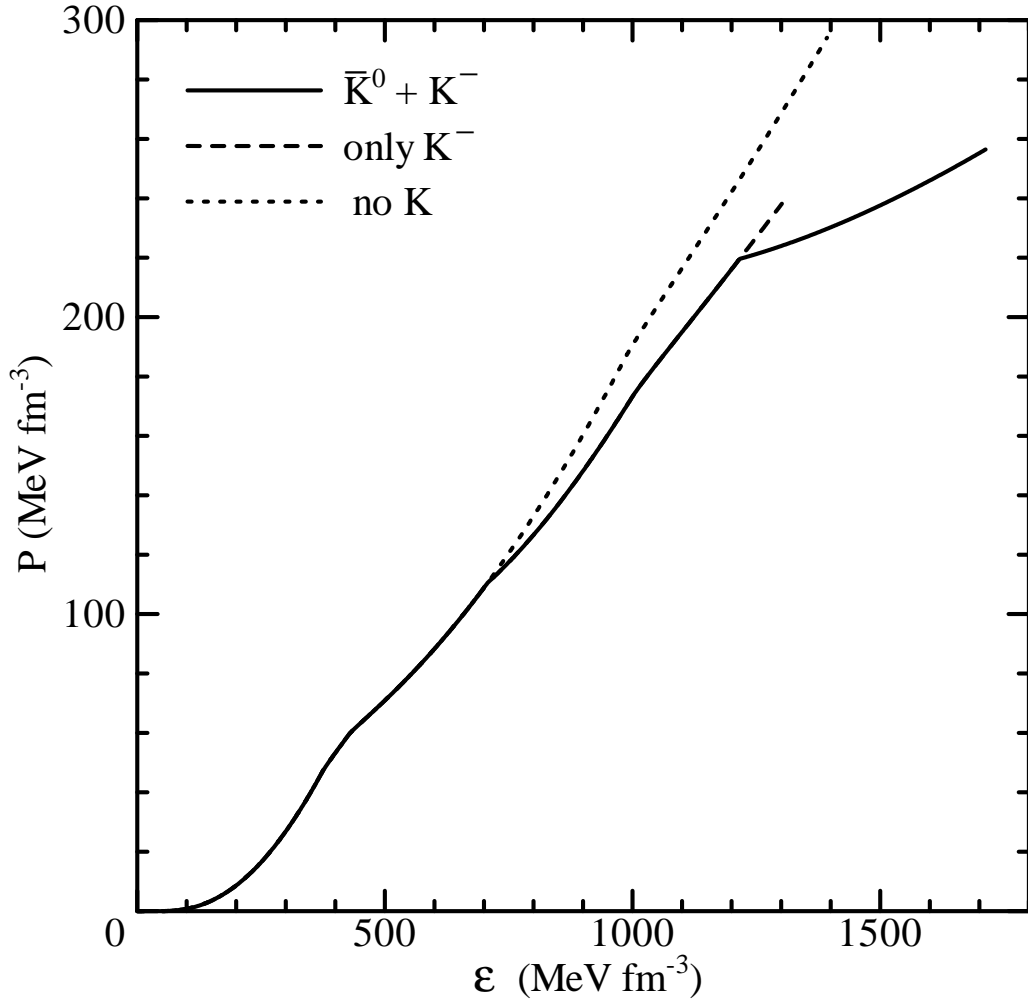


Figure 2: The equation of state (EOS) of the cold β -stable NS matter using the K^- optical potential $U_{\bar{K}}(\rho_0) = -120 \text{ MeV}$. The dashed and dotted curves are the EOS's with only K^- and no \bar{K} condensations.

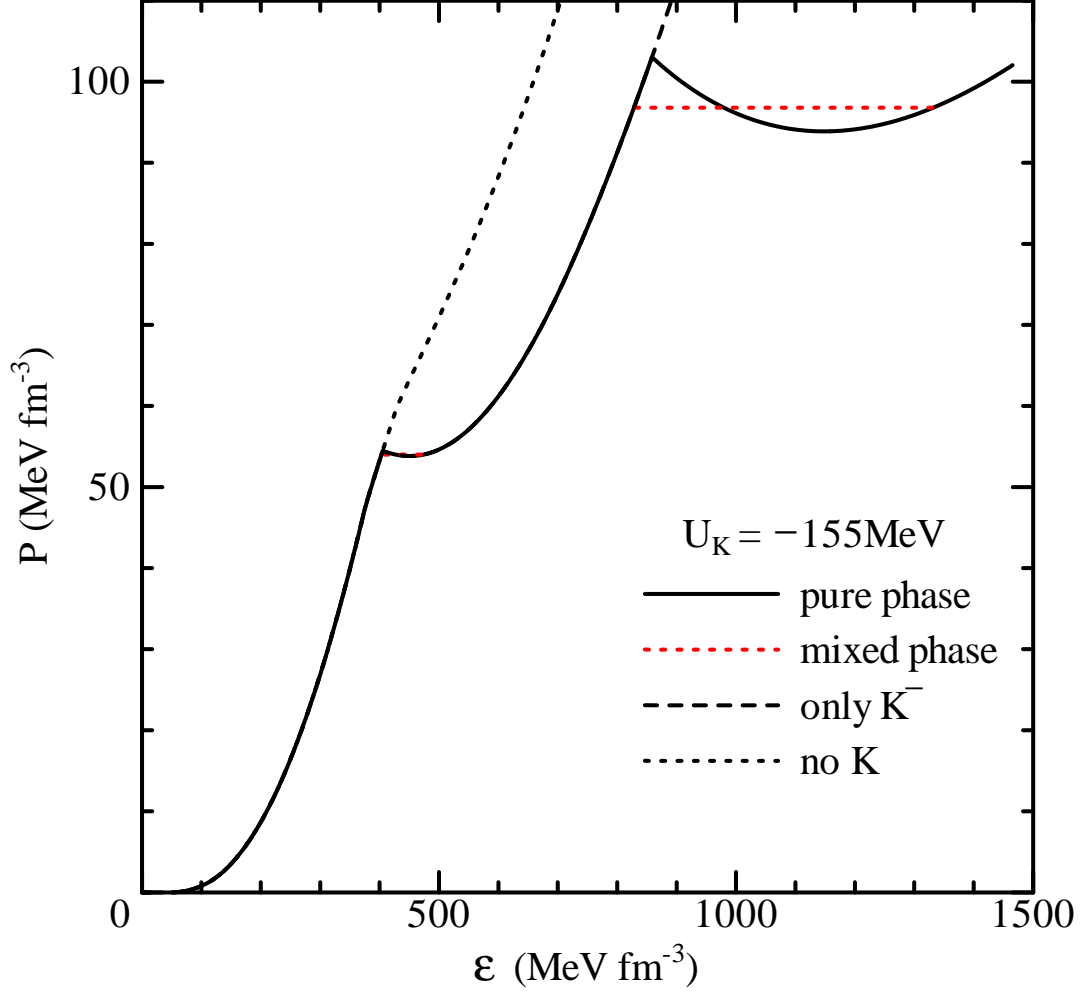


Figure 3: The equation of state (EOS) of the cold β -stable NS matter using the K^- optical potential $U_{\bar{K}}(\rho_0) = -155 \text{ MeV}$. The dashed and dotted curves are the EOS's with only K^- and no \bar{K}^0 condensations. The red dotted lines are the equilibrium states or the mixed phases of the two phases, the pure baryon and the K^- condensed phases, and the K^- and \bar{K}^0 condensed phases, respectively.

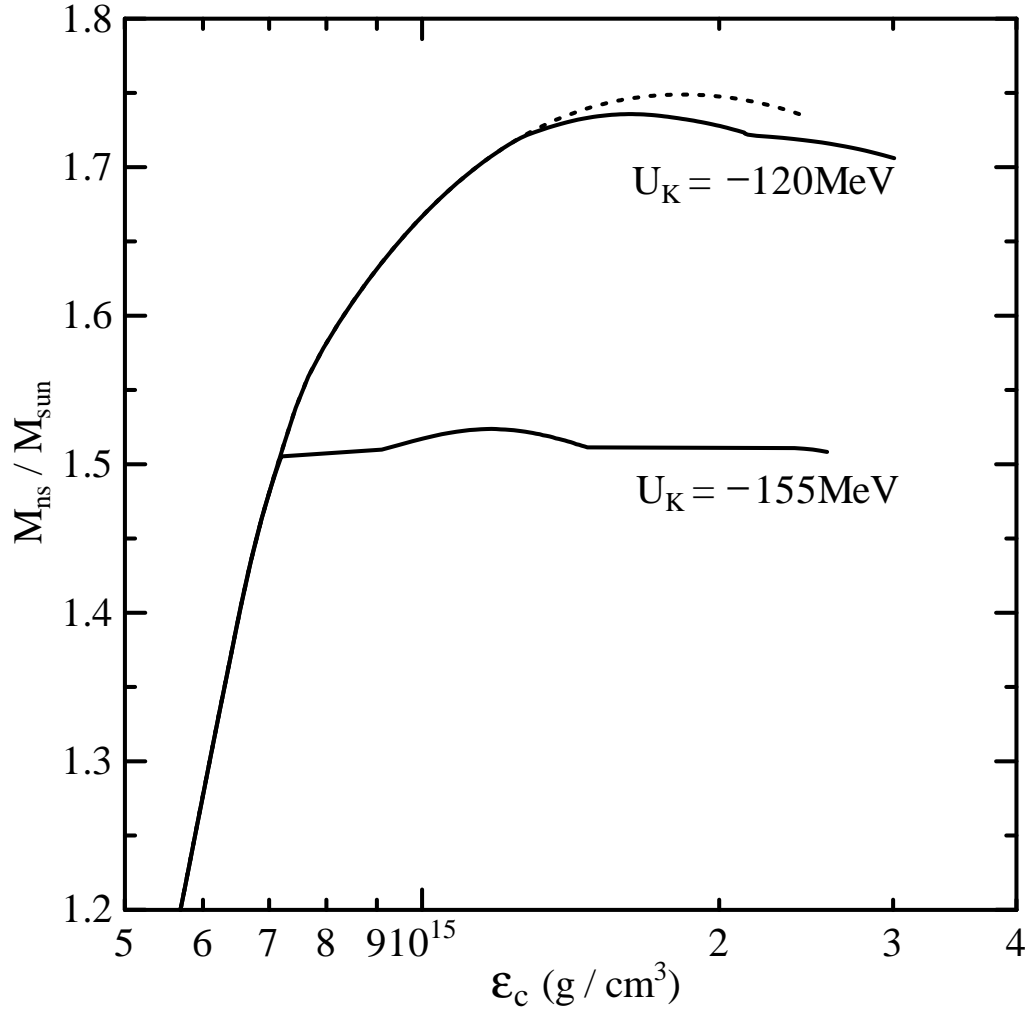


Figure 4: The mass sequences of the cold β -stable non-rotating NSs for the K^- optical potentials $U_{\bar{K}}(\rho_0) = -120$ MeV and -155 MeV. The dotted curve is the result with no antikaon condensations.

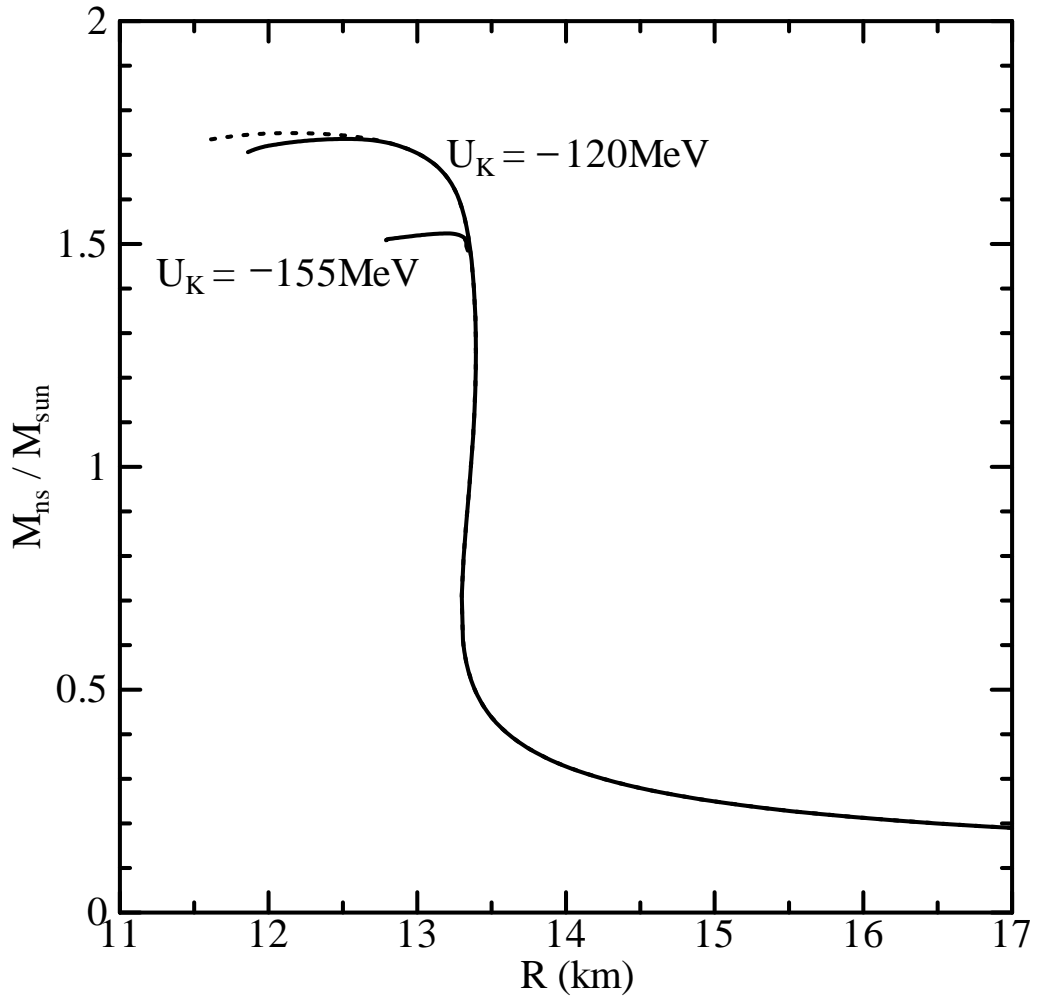


Figure 5: The mass-radius relations of the cold β -stable non-rotating neutron stars for the K^- optical potentials $U_{\bar{K}}(\rho_0) = -120$ MeV and -155 MeV. The dotted curve is the result with no antikaon condensations.